Investigating the Nature of the Hard X-ray/Soft Gamma-ray Emission from Centaurus A

James Rodi,[a,*] E. Jourdain,[b,c] M. Molina[d] and J.-P. Roques[b,c]

[a]*INAF - Istituto di Astrofisica e Planetologia Spaziali; via Fosso del Cavaliere 100; 00133 Roma, Italy*

[b]*Université de Toulouse; UPS-OMP; IRAP; Toulouse, France*

[c]*CNRS; IRAP; 9 Av. Colonel Roche, BP 44346, F-31028 Toulouse cedex 4, France*

[d]*Istituto di Astrofisica Spaziale e Fisica Cosmica di Milano; Milan, Italy*

E-mail: james.rodi@inaf.it

The question of the origin of the hard X-ray/soft gamma-ray emission in Centaurus A (Cen A) persists despite decades of observations. Low energy results from X-ray instruments suggest a jet origin. In contrast, high energy X-ray/soft gamma-ray instruments find electron temperatures indicating a corona origin is possible. The spectral energy distribution (SED) peaks in this energy range so understanding the origin of this emission is critical to modelling it. We analyzed *INTEGRAL*/IBIS-ISGRI and SPI data and observations over nearly 20 years. We did not find any spectral variability so we combined all observations for long-term average spectra. A *NuSTAR* observation was also added to study the 3.5 keV − 2.2 MeV spectrum. Spectral fits using a `CompTT` model found $kT_e \sim 520$ keV, near pair-production runaway. The spectrum was also well described by a log-parabola to model synchrotron self-Compton emission (SSC) from the jet. Using a log-parabola can explain the data up to ~ 3 GeV when including the 12-year catalog *Fermi*/LAT spectrum. Including a corona spectral component to model the hard X-rays/soft gamma-rays and a log-parabola for MeV to GeV emission can also well-describe the data, but the spectral parameters are poorly constrained. Thus, the hard X-ray/soft gamma-ray emission is likely due to SSC jet emission.

ICRC2023
38th International Cosmic Ray Conference
The Astroparticle Physics Conference

---

*Speaker

1. Introduction

As one of the brightest radio-loud active galactic nuclei (AGNs) in the hard X-ray sky, Centaurus A (Cen A) has been observed by numerous missions since its first detection in 1969 [3]. Results have shown that the spectral shape does not vary with flux [2, 4, 13, 21, 22]. But the lack of consistency in the spectral shape between different instruments has made interpreting the origin of the hard X-ray/soft gamma-ray emission difficult.

The main disagreement is over the location of spectral curvature. Analyses of lower energy instruments have found spectra well fit with a power-law model with similar spectral indexes. For example, *GRANAT*/SIGMA observations found a power-law spectrum with a slope of 1.9 ($35 - 200$ keV) with only a weak indication of a spectral break [13]. An analysis of *RXTE*/*INTEGRAL* data found a power-law spectrum with a slope of 1.83 and no spectral break [21]. [22] analysis using *RXTE* data reported a slope of 1.822 and no curvature, constraining the cutoff to > 2 MeV [22]. *XMM-Newton*/*NuSTAR* observations found an index of 1.81 and no cutoff < 1 MeV [8]. All of these spectral turnovers in the above results are well outside the energy ranges of the considered spectra and thus observations are not able to constrain the spectral break.

Observations at soft γ-ray energies have found spectral curvature, but they disagree where it occurs. OSSE/COMPTEL spectral fits in the 50 keV $-$ 30 MeV range found a spectral break at ~ 150 keV, $\Gamma_1 \sim 1.74$, and $\Gamma_2 \sim 2.0$ [24]. *INTEGRAL* observations covering $3 - 1000$ keV analyzed by [2] can be fit with $\Gamma \sim 1.7$ and $E_c \sim 400$ keV. *INTEGRAL*/SPI with *Chandra* analysis in the $2 - 500$ keV range also showed spectral curvature, with a reflection component, and $E_{cut} > 700$ keV with a confidence of $> 95\%$ [4].

Knowing the physical emission origin and the shape around the spectral energy distribution (SED) peak is important in modelling the higher energy gamma-rays to determine the origin of the excess above a few GeV [10]. Works often model it as arising from a second emission zone [10, 23, 25], which may contribute significant emission near the SED peak. Thus further constraints in that energy range can limit the possible explanations for that component.

We report on additional *INTEGRAL* observations of Cen A spanning ~ 20 years to explore the long-term temporal variability and study the soft γ-ray spectrum to investigate the high-energy spectral shape.

2. Instruments and Observations

2.1 INTEGRAL

The *INTEGRAL* satellite was launched in Oct 2002 from Baikonur, Kazachstan, with an eccentric orbit [12] that has a period of $\sim 2.5-3$ days. We analyzed data from both SPI (SPectrometer Pour INTEGRAL [27]) and IBIS/ISGRI (Imager on Board INTEGRAL/INTEGRAL Soft Gamma-Ray Imager [26]). SPI spans the 20 keV $-$ 8 MeV energy range with an energy resolution of $2 - 8$ keV [20], and ISGRI covers energies from $15 - 1000$ keV.

The SPI data were analyzed using the SPI Data Analysis Interface (SPIDAI)[1] to generate light curves and spectra (39 channels over the 20 keV to 2.2 MeV range). The data above 400 keV were

---

[1]Publicly available interface developed at IRAP to analyze SPI data. Available by contacting: spidai@irap.omp.eu. See description in Burke et al. [4]

corrected for Pulse Shape Discriminator efficiency (see the explanations and description of the appropriate procedure in [19]). The ISGRI data were analyzed with the Offline Scientific Analysis 11.2 (OSA 11.2)[2] to produce light curves and spectra, which span the $30 - 630$ keV range in 43 channels with a 1% systematic error included.

The observations used in this work span from revolution 48 to 2590 (MJD $52705 - 59948$ or 2003-03-07 to 2023-01-04) when the source was within $10°$ from the *INTEGRAL* pointing direction. It uses archival data and data from our observing campaign during *INTEGRAL*'s AO-19 observation cycle. Each observation or science window (scw) lasts $\sim 1800 - 3600$ s. Observations contaminated by solar activity and Earth's radiation belt have been removed. Finally, the total exposure time is 5.3 Ms for SPI and 4.6 Ms for ISGRI.

NuSTAR data (from both focal plane detectors, FPMA and FPMB) were reduced using the `nustardas_04May21_v2.1.1` and `CALDB` version 20220118. We used observation 60001081002, taken Aug. 6, 2013, with a cleaned exposure of ~51.3 ksec; spectral extraction and the subsequent production of response and ancillary files were performed using the `nuproducts`.

3. Results

3.1 Temporal Variability

To study the temporal behavior of Cen A, we made SPI and ISGRI light curves on an *INTEGRAL* revolution timescale ($\sim 2.5 - 3$ days). Both instruments show similar temporal evolutions, with significant flux increases between MJD 54500 and 55000. The source is significantly detected up to the $200 - 400$ keV band in SPI and in the $200 - 450$ keV band in ISGRI during the mission.

3.2 Spectral Variability

Many authors have reported that Cen A's spectrum does not change with flux [2, 4, 13, 21, 22]. In another side, *Swift*/BAT recently reported spectral softening after 2013 [17]. We searched for spectral variability in the *INTEGRAL* data by fitting the SPI $25 - 70$ keV and ISGRI $34 - 68$ keV spectra independently to a power-law model. To reduce uncertainties in the fit parameters, we grouped observations close. The photon indexes for the two instruments are consistent with a constant value, with the best-fit indexes for both instruments presenting a marginal agreement.

3.3 Average Spectrum

3.3.1 Phenomenological Models

Since no significant spectral variability was found, we combined observations for long-term average spectra to study the high-energy spectral shape of the Cen A emission. We included *NuSTAR* observations for data down to 3.5 keV. The *NuSTAR* data were fit first with an absorbed powerlaw model with absorption components for both the galactic absorption (fixed to 2.36×10^{20} cm^{-2} [11]) and an intrinsic absorption. The parameters from this fit are $\Gamma \sim 1.8$ with $n_H \sim 8.73 \times 10^{22}$ cm^{-2}. The Fe line energy is 6.36 keV with width of 0.08 keV. In later fits, the Fe line energy and width were fixed. To look for a spectral cutoff, we fit the *NuSTAR* spectra to a `zcutoffpl` model. The model better describes the data, indicating curvature is present.

Next, we applied the `zpowerlaw` model to the SPI and ISGRI data independently. The photon indexes are in perfect agreement between the two instruments for the powerlaw model. Neither spectrum was well described by the model, which over-predicted the fluxes $>\sim 150$ keV. Due to the implied presence of curvature in the spectra, we next fit the data with a cutoff power-law model. The χ^2/ν values improved. The fit parameters are in agreement between the two instruments. We performed a joint fit with the two instruments with a cross-instrument normalization with the SPI normalization fixed. The model was still an acceptable fit to the data. Subsequently, we performed a joint fit between the `NuSTAR`, SPI, and ISGRI data covering $3.5 - 2200$ keV. A cutoff power-law model finds a relatively high E_{cut} of ~ 650 keV.

The presence of reflection is an important issue since, if present and neglected, it can result in an artificially high E_{cut} [4]. We used the `pexrav` continuum model to search for a reflection component. The best-fit reflection fraction was $\sim 10^{-7}$ and consistent with 0. So, we will consider hereafter that any reflection component is negligible.

3.3.2 Physically Motivated Models

To better understand the emission mechanism(s) in this energy range, we fit the data using more physically motivated models. We first fit the data to a `CompTT` model. As pointed out in [8], the seed photon temperature is unknown, thus they fit their data to a range of seed photon temperatures with extremes of 0.05 keV and 0.5 keV. We fit our data to both values to explore a range of electron temperatures. Both fits find comparable values of $kT_e \sim 520$ keV and $\tau \sim 0.03$. An electron temperature above 500 keV disfavors a thermal origin [7].

In compact objects and in AGNs in particular, the hard X-ray/soft gamma-ray emission is potentially due to SSC jet emission. So we fit the spectra to a log parabola model, which can model the inverse Comptonization found in *Fermi* blazars (See [5] and ref within). The α value in the `log-parabola` corresponds to the slope observed at the pivot energy ($F(E) = N(E/E_{pivot})^{-\alpha-\beta log(E/E_{pivot})}$). This model also provides a good fit to the data.

More details about the data analysis and results will be given in [18].

4. Discussion

4.1 *NuSTAR/INTEGRAL* Continuum Spectrum

A joint *NuSTAR*/SPI/ISGRI fit has $E_{cut} \sim 650$ keV or $kT_e \sim 520$ keV. This again implies a corona near the runaway pair-production zone[6, 7]. These results suggest that the continuum in the hard X-ray is due to SSC emission. But, we are not able to exclude coronal emission as the dominant emission process in the hard X-ray/soft γ-ray band. For example, 3C 273 showed similar Fe line and reflection characteristics and analysis of the hard X-ray/soft gamma-ray spectrum continuum was found to be a combination of coronal plus jet emission [9, 15].

4.2 Joint Fit With Fermi/LAT

Following [15], we included *Fermi*/LAT data using the 12-year Data Release 3 catalog fluxes in 8 channels over the 50 MeV $-$ 1 TeV energy range [1]. Joint LAT/HESS analysis found a spectral

hardening at $\sim$ 3 GeV [10], whose origin remains unknown [10, 23, 25]. Thus, we included a power-law model to fit the data above 3 GeV. We tested a model where the keV to GeV emission is due to the jet (`log-par + zpowerlaw`) and found the data are well fit by the model.

Also, we tested a model where the coronal emission dominates the hard X-ray/soft γ-ray emission and the jet (SSC) component dominates in the MeV range, similar to the scenario presented for 3C 273 in [9] and [15]. We described it with a (`CompTT + log-par + zpowerlaw`) model. Some parameters are poorly constrained due to the lack of data in the MeV range and the presence of the GeV power law component, but the quality of the fit is acceptable.

Figure 1: Cen A long-term average spectra. The `CompTT+logpar+zpowerlaw` model (black dash line, with the jet component in red dotted line) and `logpar+zpowerlaw` model (cyan dot-dashed line) are overplotted.

5. Conclusion

We analyzed *INTEGRAL*/ISGRI and SPI observations of Cen A covering roughly 20 years. We first searched for spectral variability on a timescale of $\sim$ month, using the $25 - 70$ keV energy range for statistical reasons, and did not find any significant deviations from a power-law with a constant value. Building from this result, we constructed a long-term average spectrum up to 2.2 MeV. We included an observation from *NuSTAR*, which provides coverage down to 3.5 keV, to study the X-ray to soft γ-ray spectrum.

Analysis of *NuSTAR*/ISGRI/SPI spectra found a cutoff energy of $\sim$ 650 keV or $kT_e \sim 520-550$ keV. The physical interpretation of the hard X-ray/soft γ-ray emission with these values is unclear. The kT_e's are near the runaway pair-production region for the corona. Another possible scenario is emission from the jet that is well fit by a log-parabola model.

The LAT spectrum in the 50 MeV to 100 GeV range was included to the fit. A `log-par` model explains the spectrum from *NuSTAR* to LAT below $\sim$ 3 GeV as due to the jet. But, the joint spectrum can also be described by a `CompTT` component to try the presence of coronal emission in the soft X-ray to hard X-ray domain, with a `log-par` model representing the very high energy emission. The results are degenerate, but the fit parameters suggest two possible general scenarios. One where the X-ray emission is completely due to the corona and the jet emission dominates at MeV/GeV energies. The other is that the jet flux can explain the spectrum from X-rays to the GeV region. Our work favors the jet interpretation as one component can explain the whole emission from keV to LAT and the high kT_e implied by the corona scenario disfavors that interpretation. With our ongoing monitor program with *INTEGRAL*, we hope to further constrain the spectral shape of Cen A out to $\sim$ 2 MeV and possibly exclude one of the two scenarios. Polarization measurements in the MeV region by the future COSI mission may possibly differentiate the two scenarios with differing degrees of polarization between corona emission ($\sim 5 - 10\%$, [16]) and SSC emission (potentially up to $\sim 60\%$, [14]).
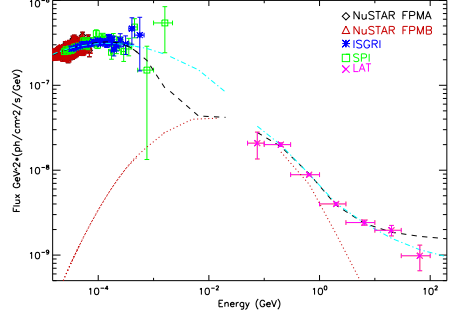
Acknowledgments

References

[1] Abdollahi, S., Acero, F., Baldini, L., et al. 2022, ApJS, 260, 53. doi:10.3847/1538-4365/ac6751

[2] Beckmann. V., Jean, P., Lubinski, P., Soldi, S., & Terrier, R. 2011, A&A, 531, A70

[3] Bowyer, C. S., Lampton, M., Mack, J., & de Mendonca, F. 1970, ApJ, 161, L1

[4] Burke, M. J., Jourdain, E., Roques, J. P., & Evans, D. A. 2014, ApJ, 787, 50

[5] Esposito, V., Walter, R., Jean, P., et al. 2015, A&A, 576, A122. doi:10.1051/0004-6361/201424644

[6] Fabian, A. C., Lohfink, A., Kara, E., et al. 2015, MNRAS, 451, 4375. doi:10.1093/mnras/stv1218

[7] Fabian, A. C., Lohfink, A., Belmont, R., et al. 2017, MNRAS, 467, 2566. doi:10.1093/mnras/stx221

[8] Fürst, F., Müller, C., Madsen, K. K., et al. 2016, ApJ, 819, 150. doi:10.3847/0004-637X/819/2/150

[9] Grandi, P. & Palumbo, G. G. C. 2004, Science, 306, 998. doi:10.1126/science.1101787

[10] H. E. S. S. Collaboration, Abdalla, H., Abramowski, A., et al. 2018, A&A, 619, A71. doi:10.1051/0004-6361/201832640

[11] HI4PI Collaboration, Ben Bekhti, N., Flöer, L., et al. 2016, A&A, 594, A116. doi:10.1051/0004-6361/201629178

[12] Jensen, P. L., Clausen, K., Cassi, C. et al. 2003, A&A, 411, L7

[13] Jourdain, E., Bassani, L., Roques, J. P., et al. 1993, ApJ, 412, 586

[14] Krawczynski, H. 2012, ApJ, 744, 30. doi:10.1088/0004-637X/744/1/30

[15] Madsen, K. K., Harrison, F. A., Markwardt, C. B., et al. 2015, ApJS, 220, 8. doi:10.1088/0067-0049/220/1/8

[16] Matt, G. 1993, MNRAS, 260, 663. doi:10.1093/mnras/260.3.663

[17] Rani, B., Mundo, S. A., Mushotzky, R., et al. 2022, ApJ, 932, 104. doi:10.3847/1538-4357/ac6fd4

[18] Rodi, J., Jourdain, E., Molina, M. & Roques, J.-P. , submitted

[19] Roques, J.-P. & Jourdain, E. 2019, ApJ, 870, 92. doi:10.3847/1538-4357/aaf1c9

[20] Roques, J. P., Schanne, S., von Kienlin, A. et al. 2003, A&A, 411, L91

[21] Rothschild, R. E., Wilms, J., Tomsick, J., et al. 2006, ApJ 641, 801

[22] Rothschild, R. E., Markowitz, A., Rivers, E., et al. 2011, ApJ, 733, 23

[23] Joshi, J. C., Miranda, L. S., Razzaque, S., et al. 2018, MNRAS, 478, L1. doi:10.1093/mnrasl/sly064

[24] Steinle, H., Bennett, K., Bloemen, H., et al. 1998, A&A, 330, 97

[25] Tanada, K., Kataoka, J., & Inoue, Y. 2019, ApJ, 878, 139. doi:10.3847/1538-4357/ab2233

[26] Ubertini, P., Lebrun, F., Di Cocco, G., et al. 2003, A&A, 411, L131. doi:10.1051/0004-6361:20031224

[27] Vedrenne, G., Roques, J.-P., Schönfelder, V., et al. 2003, A&A, 411, L63. doi:10.1051/0004-6361:20031482

PoS(ICRC2023)650